Cancer Management and Research

Dovepress

open access to scientific and medical research

Open Access Full Text Article

ORIGINAL RESEARCH

Knocking Out *SST* Gene of BGC823 Gastric Cancer Cell by CRISPR/Cas9 Enhances Migration, Invasion and Expression of SEMA5A and KLF2

This article was published in the following Dove Press journal:
Cancer Management and Research

Wei Chen[1]
Ruixian Ding[1]
Jinlu Tang[1]
Haodong Li[2]
Chonghua Chen[2]
Yaru Zhang[1]
Qinxian Zhang[1]
Xiaoyan Zhu[1]

[1]Department of Histology and Embryology, School of Basic Medical Sciences, Zhengzhou University, Henan, People's Republic of China; [2]Department of Clinical Medicine, School of Basic Medical Sciences, Zhengzhou University, Henan, People's Republic of China

Background: The impact and potential molecular mechanisms of SST in the occurrence and development of GC have not been determined.

Materials and Methods: Two pairs of sgRNA and reporter were designed according to targeting sequence of SST gene for double-nicking. Plasmids were transfected into 293T for selecting sgRNA with higher cutting efficiency. The subline which has knocked-out *SST* gene were selected by FACS and verified by sequencing and expression level. Moreover, the migration and invasion ability was evaluated by wound healing and transwell after knocking out SST. Besides, the protein expression of SEMA5A and KLF2 were observed by Western blotting and LSCM. Last, we detected the expression levels of SST, SEMA5A, and KLF2 in GC tissues by Western blotting.

Results: The results revealed that the new subline 1E9, which had knocked out *SST* gene, was established by CRISPR/Cas9. In addition, the knockout of SST in GC cells markedly increased migration and invasion ability. The results also demonstrated that the knockout of SST increased the expression of SEMA5A and KLF2. The expression level of SST was decreased in GC tissues, and its decrease was associated with overexpression of SEMA5A and KLF2.

Conclusion: SST plays an inhibitory role in the migration and invasion of GC cell BGC823. The protein expression levels of SEMA5A and KLF2 were enhanced in GC cells and tissues lacking SST expression.

Keywords: somatostatin, CRISPR/Cas9, gastric cancer, migration, invasion

Introduction

Gastric cancer (GC) is the fifth most common cancer with 8.2% mortality in the world.[1] Despite many improvements in the treatment of this disease, the survival rate remains poor, especially for patients accompanying with lymphatic metastasis.[2] Therefore, a better understanding of the molecular mechanisms underlying the progression and tumour metastasis of GC is of great importance for its therapies. GC is a type of tumour that is relatively sensitive to hormones, such as thyroid hormones.[3] Somatostatin (SST), a cyclic peptide hormone, affects growth hormone secretion, gastrointestinal tract movement, and blood flow in the digestive tract.[4] SST also affects the occurrence and development of cancer. SST and chemokine CXCR4 may represent a promising therapeutic strategy in pancreatic adenocarcinoma.[5] There are also some new SST analog drug could target the pancreatic cancer.[6] Besides, SST also contributes to quiescence of stem cells and

Correspondence: Xiaoyan Zhu
Department of Histology and Embryology, School of Basic Medical Sciences, Zhengzhou University, No. 100 Science Road, Henan 450000, People's Republic of China
Tel +86 139 3829 0386
Fax +86 371 6778 1953
Email zhxy@zzu.edu.cn

submit your manuscript | www.dovepress.com
DovePress
http://doi.org/10.2147/CMAR.S236374

inhibition of proliferation of colon cancer.[7] Some research show that the expression of SST has a certain correlation with the occurrence and development of GC.[4,8] However, the role and function mechanism of SST on GC have not clarified. To explore the role of genes in cancer, genome-editing technology was applied for the purpose of gene knockout or mutation. Compared to zinc finger nucleases (ZFNs) and transcription activator-like effector (TALE)-nucleases (TALENs), the CRISPR/Cas9 system performs a highly site-specific double-strand break, which means more precise gene knockout.[9]

Semaphorin 5A (SEMA5A) is a member of the Semaphorin family identified as an axonal guidance factor during the development of the central nervous system.[10] However, growing evidence indicates that SEMA5A is expressed in many tissues besides the nervous system and has additional functions. Noticeably, certain SEMAs have been found to play a regulatory role in tumourigenesis and the process of tumour formation.[11,12] KLF2 is a member of the Krüppe-like factors (KLFs), a large family of DNA-binding transcriptional regulators[13] that play important roles during the growth and differentiation processes of epithelial cells.[14] The KLFs family members have been considered as tumour suppressors in cancer for their inhibitory effects on cell proliferation.[15] While it has been reported that KLF2 plays different roles in cancer according to different tissue and pathways.[16] Few investigations and studies have been performed on the potential roles and expression of SEMA5A and KLF2 in human tumours including GC.

This study detected the expression of SST, SEMA5A, and KLF2 in GC, indicating that SEMA5A and KLF2 may interrelate with SST during the development of GC.

Materials and Methods

Patients and Specimens

A total of five pairs of human GC and normal tissues were obtained from Henan Cancer Hospital (Zhengzhou, Henan, China). All samples were obtained with patients' informed consents.

Cell Lines and Culture

293T and GC cell line BGC823 was purchased from the Chinese Academy of Science cell bank (Shanghai, China). 293T was cultured in DMEM medium (HyClone, USA) with 10% fetal bovine serum (BI, Israel) and 1% penicillin-streptomycin (Solarbio, China) at 37°C containing 5% CO2。 BGC823 was cultured in PRIM 1640 medium (HyClone, USA) with 10% fetal bovine serum and 1% penicillin-streptomycin at 37°C containing 5% CO2。

Plasmid Construction and Transfection

Six pairs sgRNA targeting exon 1 of gene SST were designed using the website http://crispr.mit.edu, and 2 pairs of reporters containing sgRNAs and TAA were designed by NTI (Table 1). Then, the sgRNA linked to px330 which expresses Cas9,[17] and the reporters linked to pmCherry-EGFP. Figure 1A shows the schematic diagram of pmCherry-EGFP-reporter. Target plasmids were extracted after px330-sgRNA or pmCherry-EGFP-reporter transfecting competent *E. coli* DH5 α(TAKARA, Dalian, China) and was detected by 0.8% agarose gel to confirm whether plasmids were constructed successfully. Cells were cultured in 24-well plate overnight. 0.8 μg plasmid were transfected with 2 μL Lipofectamine 2000 reagent (Invitrogen, USA) according to the manufacturer's instructions.

Flow Cytometry and Fluorescence-Activated Cell Sorting (FACS)

The cells were digested and resuspended in cold PBS. The fluorescence intensity of transfected cells was measured using the Accuri C6 (BD, CA, USA), and data were analyzed using FACS Calibur (BD, CA, USA). The isotype controls were used to set the gates for positive and negative populations. Targeted single cells were sorted by FACSAria (BD, CA, USA) and cultured in PRIM-1640 with 20% FBS.

Sequencing

DNA of cells was extracted and then analysed by PCR. Primers were designed according to the target sequence, then PCR product was extracted from the gel for sequencing. Forward Primer: CTTTAGGAGCGAGGTTCGGA; Reverse Primer: AGGACTGAGCATCCCTTAGG.

Immunocytochemistry

Cells were grown on cover glasses and fixed with 4% paraformaldehyde for 20 mins at room temperature, permeabilized with 0.5% Triton X-100 for 10 mins and blocked with goat serum for 20 mins. After that, cells were incubated with primary antibody SST (ab183855, Abcam, 1:100) overnight. Cells were then washed with PBST and incubated with HRP-IgG secondary antibody at 37°C for 20 mins, followed by coloration with 3,3-

Table 1 Sequence of sgRNA and Reporter

PRIMER	SEQUENCE
SST sgRNA-1F	CACCggctgcgctgtccatcgtcc
SST sgRNA-1R	AAACggacgatggacagcgcagcc
SST sgRNA-2F	CACCgctgtgtcaccggcgctccct
SST sgRNA-2R	AAACagggagcgccggtgacacagc
SST sgRNA-3F	CACCgctgccgcctccagtgcgcgc
SST sgRNA-3R	AAACgcgcgcactggaggcggcagc
SST sgRNA-4F	CACCgagtccctggctgctgccgcg
SST sgRNA-4R	AAACcgcggcagcagccagggactc
SST sgRNA-5F	CACCgaagtccctggctgctgccgc
SST sgRNA-5R	AAACgcggcagcagccagggacttc
SST sgRNA-6F	CACCgaagtccctggctgctgccg
SST sgRNA-6R	AAACcggcagcagccagggacttc
SST reporter-1F	TCGACtcctgccgcctccagtgcgcgctggctgcgctgtccatcgtcctggccctgggct gtgtcaccggcgctccctcTAAC
SST reporter -1R	AATTGTTAgagggagcgccggtgacacagcccagggccaggacgatggacagc gcagccagcgcgcactggaggcggcaggaG
SST reporter -2F	TCGACttctgcagaagtccctggctgctgccgcggggaagTAAC
SST reporter -2R	AATTGTTActtccccgcggcagcagccagggacttctgcagaaG

Notes: The blue bases are the stop codon sequence, and the yellow bases are the sticky end, among them the red bases are the base modified at the end.

diaminobenzidine (DAB), kept at room temperature without light for approximately 1 min and the coloration ended with distilled water. After haematoxylin staining, slides were dehydrated with sequential ethanol washes of 1 min each starting with 50%, 75%, followed by 80% and finishing with a 100% ethanol wash. Slides were sealed and imaged by microscope.

Wound-Healing Assay

Cells were plated in 12-well plates and incubated to a density of 80%. Then, cells were scratched with 200 μL pipette tips and washed twice with PBS softly. Serum-free medium was applied to culture cells for 48 hrs. The wound areas were imaged by microscope (Olympus, Tokyo, Japan) at 0 hrs, 24 hrs and 48 hrs. We measured the scratch area by Image J, and calculated the wound-healing percentage. Wound-healing percentage $= \frac{\text{scratch area at 0h} - \text{scratch area at 24h or 48h}}{\text{scratch area at0h}} * 100$.

Transwell Assay

Transwell chambers (Corning, NY, USA) were precoated with diluted matrigel (1:4, BD Biosciences, USA) and incubated at 37°C for 2 hrs. Cells (5×10^4 cells per well) without serum were added to the upper chamber, and the lower chamber was filled with 750 μL completed PRIM-1640 medium containing 15% FBS. The chambers were incubated at 37°C for 24 hrs. Then, the invaded cells were counted after staining with crystal violet and imaged by microscope (Olympus, Tokyo, Japan).

Western Blotting

Total protein was lysed in RIPA (Solarbio, Beijing, China) and quantified by BCA assay kit (Solarbio, Beijing, China). Then, proteins were separated by 12% SDS-PAGE and transferred to PVDF (Millipore, USA). After being blocked by 5% nonfat milk for 2 hrs at room

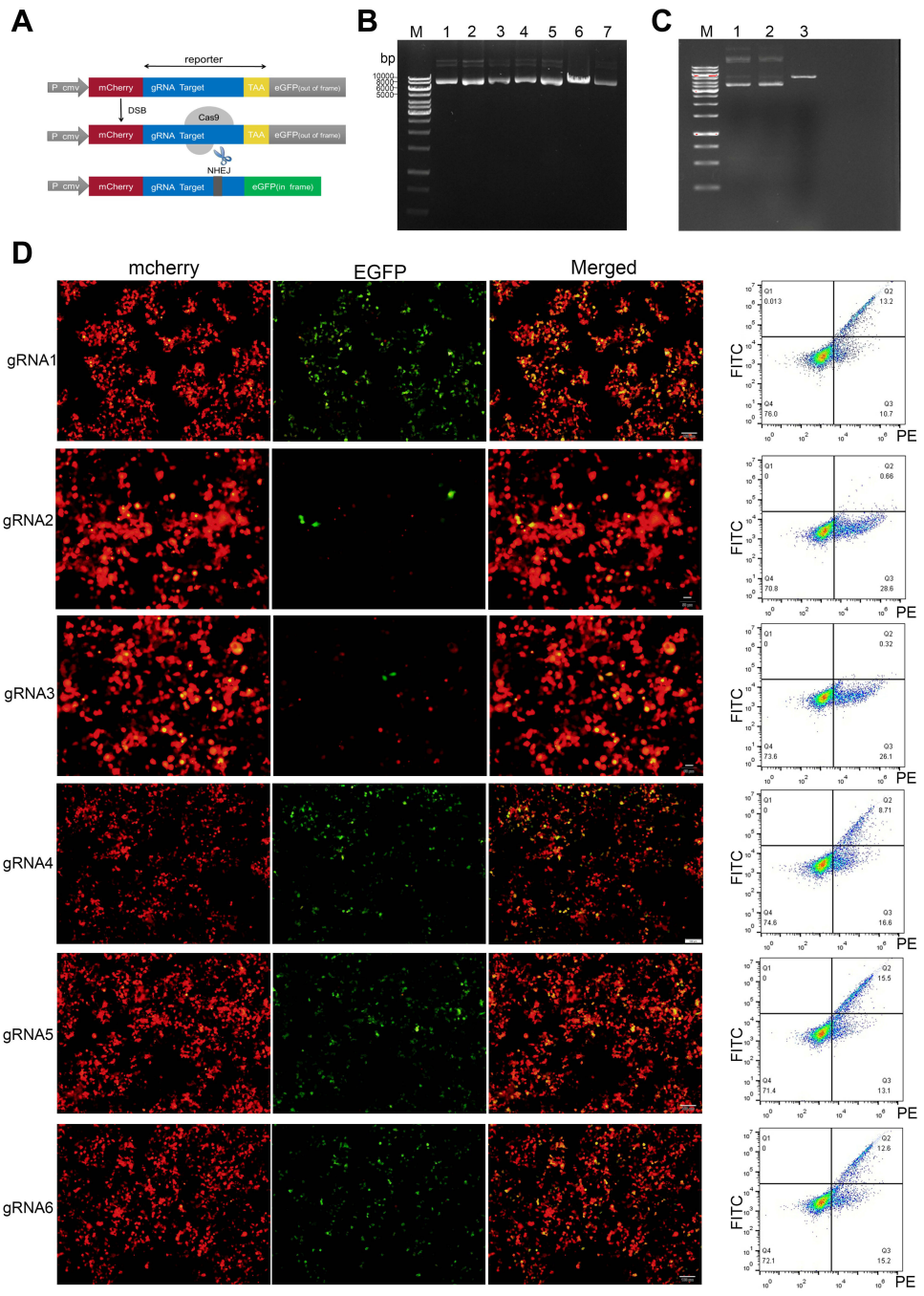

Figure 1 Construction of plasmids and selection of suitable sgRNA. (**A**) Schematic diagram of pmCherry-EGFP-reporter. (**B**) Carrying out electrophoresis after the vectors px330-SST-sgRNA were digested by enzyme. In-line 6, a band appeared at approximately 8500 bp. Lines 1, 2, 3, 4, 5, and 7, three bands appeared. The results showed that the recombinant vectors were circular and successfully constructed. (**C**) Carrying out electrophoresis after the vectors pmCherry-EGFP-SST-reporter were digested by restriction enzyme. In-line 3, a band appeared at approximately 5400 bp, Lines 1 and 2, three bands appeared. The results showed that the recombinant vectors were circular and successfully constructed. (**D**) The vectors pmCherry EGFP-SST-reporter and px330-SST-sgRNA were co-transfected into 293T cells. As shown by fluorescence microscope and flow analysis, the amount of cells with green fluorescent expression represents the efficacy of sgRNA.

temperature, the membranes were incubated with primary antibody overnight at 4°C.Primary antibody included SST (ab183855, Abcam, 1:1000), SEMA5A (AF5896, R&D, 1 μg/mL), KLF2 (ab20359, Abcam, 1:500) and β-actin (4970, CST, 1:1000). Then, the membranes were incubated with appropriate secondary antibody for 2 hrs at room temperature. At last, protein bands visualized using ECL reagent (Beyotime, Shanghai, China).

Immunofluorescence

Immunofluorescence was performed as described below. Cells were fixed with 4% paraformaldehyde for 20 mins at room temperature, permeabilized with 0.5% Triton X-100 for 10 min and blocked with 1% bovine serum albumin–phosphate-buffered saline with Tween 20 for 2 hrs. After that, cells were incubated with primary antibodies KLF2 (MAB5466, R&D, 20μg/mL) and SEMA5A (AF5896, R&D, 10μg/mL) overnight. Then, the cells were washed with PBST and incubated with Donkey Anti-Mouse IgG (Alexa Fluor 647, Abcam) and Donkey Anti-Sheep IgG (Alexa Fluor 488, Abcam). All images were captured with a laser scanning confocal microscope (Olympus).

Statistical Analysis

Significance tests were performed using GraphPad Prism 5.0. The statistical significance of differences between the groups was determined using two-tailed Student's *t*-test. $P<0.05$ was considered significant.

Results

CRISPR/Cas9 Double-Nicking Vectors Were Constructed

After successful construction, the vectors were digested by the restriction enzymes BbsI and EcoRI, then the product was electrophoresed on agarose gels. As seen in Figure 1B, vector px330 only appeared as a band of approximately 8500 bp (Line 6), px330-SST-sgRNA1 to px330-SST-sgRNA6 (Lines 1, 2, 3, 4, 5, 7) appeared as three bands, indicating that the recombinant vector was circular, that is, the vectors were successfully established. In addition, as shown in Figure 1C, the vector pmCherry-EGFP appeared as a band of approximately 5400 bp (Line 3), pmCherry-EGFP-SST-reporter1-2 (Line 1–2) appeared as three bands, owing to the change of the last base in the cohesive end of the reporter; therefore, the recombinant vector would be circular, similar to px330-SST-sgRNA. These results indicated that the vectors were successfully constructed. To seek out the sgRNA with highest cutting efficiency from three pairs of sgRNAs at two different cleavage sites, we transfected sgRNA1 or sgRNA2 or sgRNA3 and reporter1; sgRNA4 or sgRNA5 or sgRNA6 and reporter2 into 293T cell. According to the amount of EGFP expression in cells, sgRNA1 and sgRNA5 had the highest cutting efficiency and were selected for next experiments (Figure 1D).

Sublines Were Obtained by FACS and Verified

After FACS, target single cells were cultured until they formed monoclonal cell populations (Figure 2A). The monoclonal cell genome was extracted and amplified by PCR, and the PCR product was subjected to agarose gel electrophoresis. As seen in Figure 2B, the PCR product of BGC823 was approximately 330 bp, and the PCR product of the sublines appeared with different bands. In-line 9, a band appeared at approximately 240 bp, while in other lines two bands appeared at approximately 240 bp and 330 bp or none. This result indicated that when the sgRNA guided Cas9 to double-cleave, it would cut off approximately 90 bases, the subline 1E9 (Line 9) was composed of homozygous cells and *SST* gene was successfully knocked out. Lines, where two bands appear, may be due to heterozygous cells (Figure 2B). The sequencing results of the 1E9 PCR product showed that approximately 90 bases were deleted compared with BGC823 PCR product. The deletion site was identical to the targeted knockout site, indicating that *SST* gene target site was deleted, and the frame shift mutation was caused (Figure 2C). Furthermore, the expression of SST in BGC823 and 1E9 was also explored via immunocytochemistry and Western blotting. The results indicated that the obtained subline 1E9 had no SST expression (Figure 2D and E).

SST Inhibits the Invasion and Migration of Gastric Cancer

As invasion and migration are two key hallmarks of cancer,[18] we performed transwell and wound-healing assays to determine the effect of SST on the invasion and migration ability of GC cells. The results showed that 1E9 promotes invasion and migration ability than BGC823 (Figure 3A and B). These data revealed 1E9 that knocking out SST enhanced the ability of GC cells to invade and migrate, indicating that SST could influence GC carcinogenesis by inhibiting cancer cell invasion and migration.

Expression of SST Negatively Correlates with SEMA5A and KLF2

To further investigate the potential mechanism by which SST inhibits the progression of GC, immunofluorescence, and

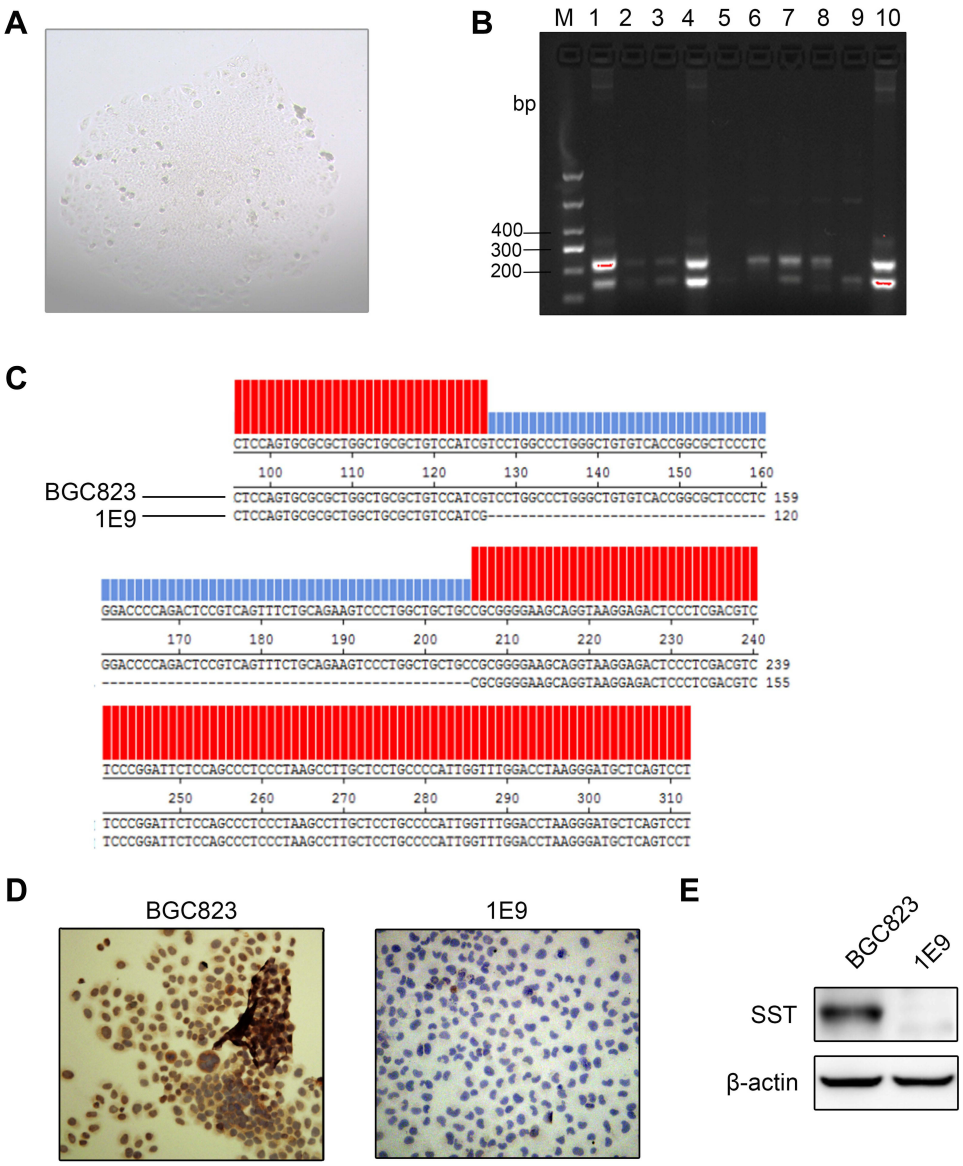

Figure 2 Establish of cells knocking out *SST* gene. (**A**) The monoclonal cell population had formed. (**B**) Performance of electrophoresis after PCR, with the results showing that the PCR product appears as different bands. In-line 6, a product of BGC823 cells appears as a single band at 330 bp. In-line 9, a product of 1E9 subline appears as a single band of 240 bp. (**C**) The PCR product of the 1E9 was sequenced. Red part has the same bases as BGC823, and the blue one represents the deletion of bases compared to BGC823 cells. (**D**) The protein levels of SST were detected by immunofluorescence in BGC823 and 1E9. (**E**) The protein levels of SST were detected by Western blotting in BGC823 and 1E9.

Western blotting was performed to detect the expression of SEMA5A and KLF2. For immunofluorescence, laser scanning confocal-microscopy was used to observe the fluorescence. In GC cells, SEMA5A was expressed in the nucleus and KLF2 localized to the nucleus and cytoplasm. The results of the immunofluorescence showed that the expression of SEMA5A and KLF2 was significantly higher in subline 1E9 compared to BGC823. The results of Western blotting were consistent with the immunofluorescence (Figure 4A and B). We also detected the expression level of SST in five pairs GC and normal tissues. It showed that the expression of SST is decreased in GC. While the expression of SEMA5A and KLF2 was higher in GC compared to normal tissues (Figure 4C). Taken together, these results provide evidence that SST may negatively interrelate with SEMA5A and KLF2 during the occurrence and progression of GC.

Discussion

To investigate the effect of SST on the development of GC, most previous studies determined the clinical significance of SST and the SST receptor (SSTR) on GC cell by measuring the expression level of SST and SSTRs in GC tissue

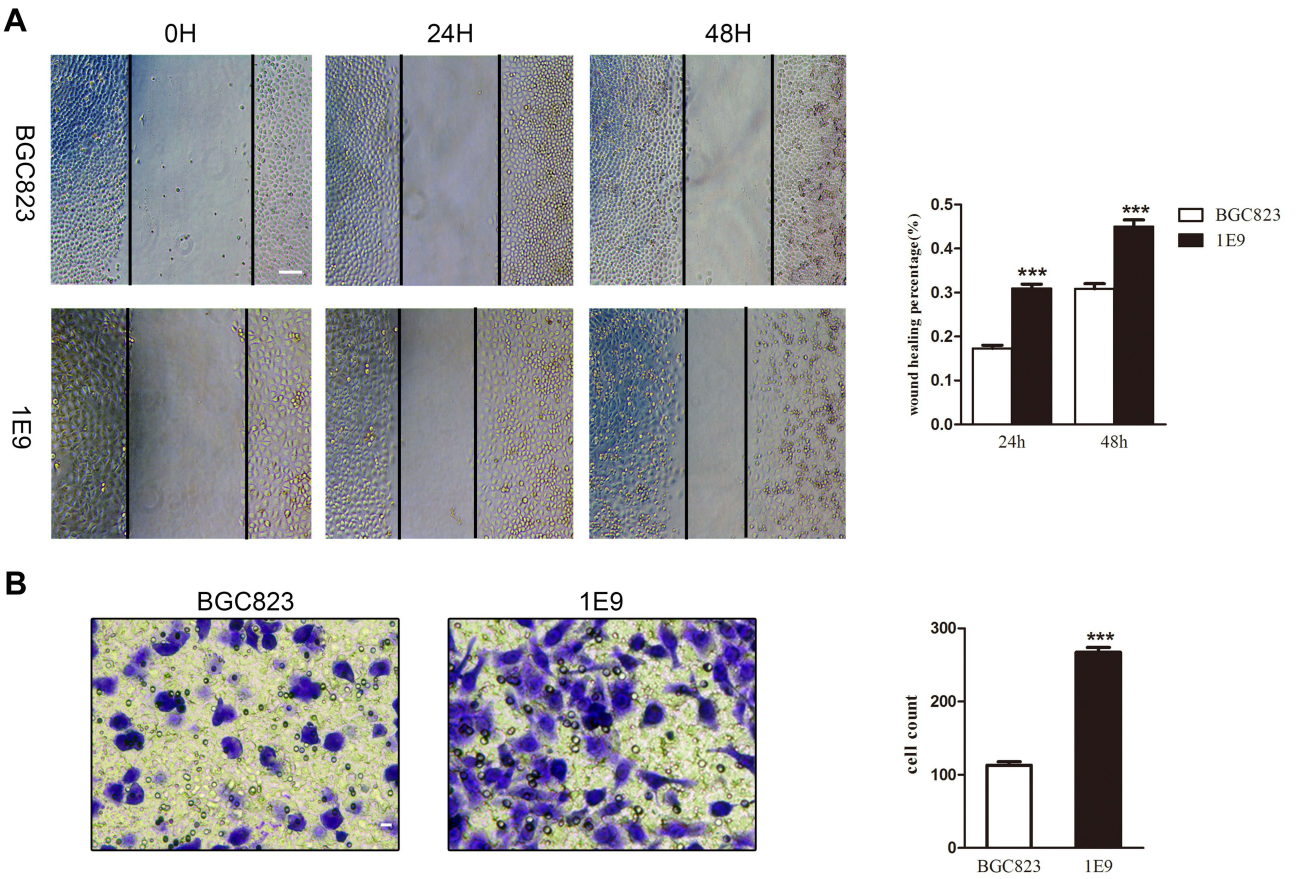

Figure 3 The migration and invasion abilities of 1E9 were higher than BGC823. (**A**) Cells were plated and wounded. Photographs were taken after 0, 24, and 48 hrs (***P<0.001 according to the two-tailed t test, scale bar 100 μm). (**B**) The number of invaded cells was counted in three random fields. Representative images of invaded cells were shown (***P<0.001 according to the two-tailed t test, scale bar 40 μm). Data are presented as mean±s.d. from three independent experiments.

samples.[19,20] There is less evidence on molecular mechanisms for the development of SST in GC. RNA interference (RNAi) has been used in the study of mechanism.[21] Furthermore, because of the presence of off-target effects and low-efficiency, RNAi technology could cause non-specific silencing.[22] Compared to the new generation of genetic editing technology, CRISPR/Cas9, RNAi blocks protein production by blocking mRNA, while CRISPR/Cas9 works at an earlier step in the process of cellular protein production, genetically modifying at the DNA level to prevent the transcription and translation of DNA. CRISPR/Cas9 can perform site-specific knockout and insertion of genes compared to ZFN and TALEN gene-editing systems. In this experiment, we designed two pairs of sgRNAs to bind two different sites of the target sites to reduce off-target activity and improve specificity,[23] and we used a modified Cas9 endonuclease to create a double nick system; in addition, we designed multiple pairs of sgRNAs for preliminary screening. All these steps further improved the efficiency and accuracy of the gene knockout.

We performed single cell sorting using FACS to ensure the monoclonality of the cells. The homozygous monoclonal sublines were verified using sequencing. The immunocytochemistry and Western blotting results showed 1E9 cells expressed no SST protein, indicating that after knocking out, the gene sequence was frame shifted and the encoded protein was altered. Furthermore, the invasion and migration abilities of 1E9 subline were significantly increased compared to BGC823 cells, indicating that knocking out *SST* gene has a certain influence on the invasion and migration of GC cells. Invasion and migration are important features of malignant tumors. The findings reveal that SST can inhibit the invasion and migration of GC cells. Besides, the expression of SST in GC tissues is decreased significantly compared to normal tissues. All results show that SST plays a certain inhibitory role in the development of GC.

A previous study has shown that KLF2 inhibits the growth and migration of GC cells by inducing the expression of PTEN at both mRNA and protein levels. KLF2 also significantly inhibits AKT-mTOR signalling downstream of

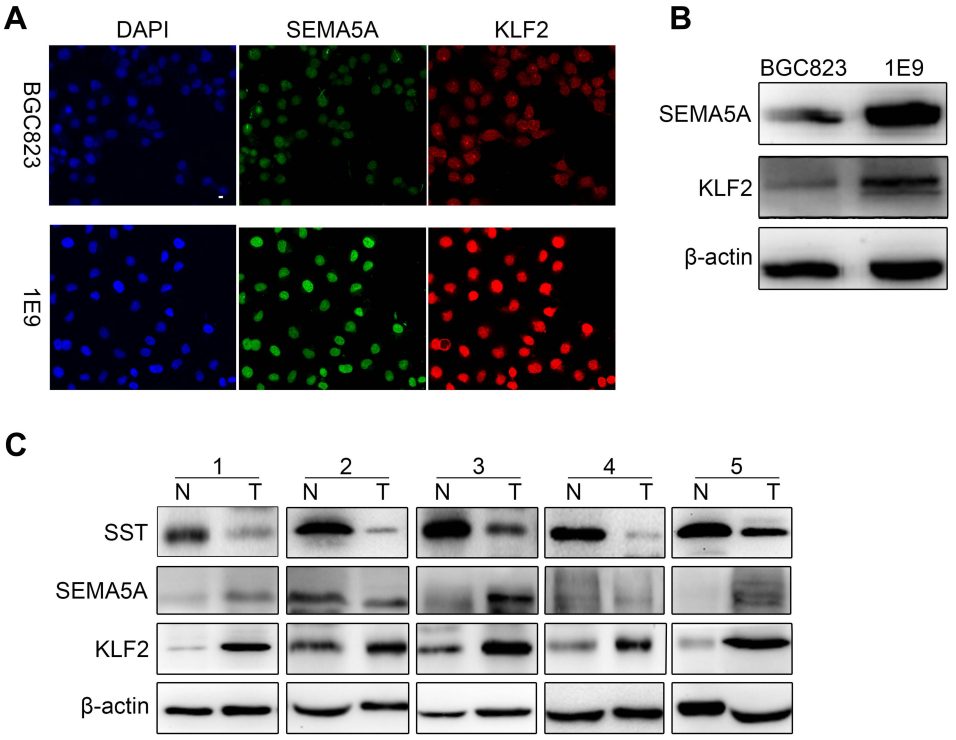

Figure 4 Expression of SST negatively correlates with SEMA5A and KLF2. (**A**) The protein levels of SEMA5A and KLF2TECs were detected by immunofluorescence in BGC823 and 1E9. (**B**) The protein levels of SEMA5A and KLF2 were detected by Western blotting in BGC823 and 1E9. (**C**) The protein levels of SST, SEMA5A, and KLF2 were detected by Western blotting in five pairs GC and normal tissues.

PTEN. The AKT-mTOR signalling pathway inhibits cell proliferation and promotes apoptosis to some extent.[24,25] SEMA5A may mediate the invasion and metastasis of GC cells by activating TGFβ1 and relying on ERK1/2 to upregulate the expression of uPA and MMP-9.[26] Studies have confirmed that the combination of different elements of KLF2 causes different downstream signaling to play different roles for tumor cells.[27] In our experiments, knocking out *SST* gene promoted the migration and invasion of GC cells. Meanwhile, the protein expression levels of SEMA5A and KLF2 were enhanced in GC cells and tissues lacking SST expression. It can provide some evidence about the relationship between SST and SEMA5A or KLF2 during the occurrence and progression of GC.

Data Sharing Statement

The datasets supporting the conclusions of this article are included in this article and its additional images. Raw data are available from the corresponding author on reasonable request.

Acknowledgment

This study was supported by a grant from the project of Henan Provincial Science and Technology Project (NO.172102310089, NO.172102310112) and 2018 College Student Innovation Experiment Project of Henan Province (NO.201810459078).

Author Contributions

All authors contributed to data analysis, drafting or revising the article, gave final approval of the version to be published, and agree to be accountable for all aspects of the work.

Disclosure

The authors report no conflicts of interest in this work.

References

1. Bray F, Ferlay J, Soerjomataram I, Siegel RL, Torre LA, Jemal A. Global cancer statistics 2018: GLOBOCAN estimates of incidence and mortality worldwide for 36 cancers in 185 countries. *CA Cancer J Clin*. 2018;68(6):394–424. doi:10.3322/caac.21492
2. Siegel R, Ma JM, Zou ZH, Jemal A. Cancer statistics, 2014. *CA Cancer J Clin*. 2014;64(1):9–29. doi:10.3322/caac.21208
3. Brown AR, Simmen RCM, Simmen FA. The role of thyroid hormone signaling in the prevention of digestive system cancers. *Int J Mol Sci*. 2013;14(8):16240–16257. doi:10.3390/ijms140816240
4. Shi X, Li X, Chen L, Wang C. Analysis of somatostatin receptors and somatostatin promoter methylation in human gastric cancer. *Oncol Lett*. 2013;6(6):1794–1798. doi:10.3892/ol.2013.1614

5. Kajtazi Y, Kaemmerer D, Sanger J, Schulz S, Lupp A. Somatostatin and chemokine CXCR4 receptor expression in pancreatic adenocarcinoma relative to pancreatic neuroendocrine tumours. *J Cancer Res Clin Oncol*. 2019;145(10):2481–2493. doi:10.1007/s00432-019-03011-0
6. Ragozin E, Hesin A, Bazylevich A, et al. New somatostatin-drug conjugates for effective targeting pancreatic cancer. *Bioorg Med Chem*. 2018;26(13):3825–3836. doi:10.1016/j.bmc.2018.06.032
7. Modarai SR, Opdenaker LM, Viswanathan V, Fields JZ, Boman BM. Somatostatin signaling via SSTR1 contributes to the quiescence of colon cancer stem cells. *BMC Cancer*. 2016;16(1):941. doi:10.1186/s12885-016-2969-7
8. Stollberg S, Kammerer D, Neubauer E, et al. Differential somatostatin and CXCR4 chemokine receptor expression in MALT-type lymphoma of gastric and extragastric origin. *J Cancer Res Clin Oncol*. 2016;142(11):2239–2247. doi:10.1007/s00432-016-2220-6
9. Maeder ML, Gersbach CA. Genome-editing technologies for gene and cell therapy. *Mol Ther*. 2016;24(3):430–446. doi:10.1038/mt.2016.10
10. Matsuoka RL, Chivatakarn O, Badea TC, et al. Class 5 transmembrane semaphorins control selective mammalian retinal lamination and function. *Neuron*. 2011;71(3):460–473. doi:10.1016/j.neuron.2011.06.009
11. Rehman M, Tamagnone L. Semaphorins in cancer: biological mechanisms and therapeutic approaches. *Semin Cell Dev Biol*. 2013;24(3):179–189. doi:10.1016/j.semcdb.2012.10.005
12. Roth L, Koncina E, Satkauskas S, Cremel G, Aunis D, Bagnard D. The many faces of semaphorins: from development to pathology. *Cell Mol Life Sci*. 2009;66(4):649–666. doi:10.1007/s00018-008-8518-z
13. McConnell BB, Yang VW. Mammalian Kruppel-like factors in health and diseases. *Physiol Rev*. 2010;90(4):1337–1381. doi:10.1152/physrev.00058.2009
14. Cao Z, Sun X, Icli B, Wara AK, Feinberg MW. Role of Kruppel-like factors in leukocyte development, function, and disease. *Blood*. 2010;116(22):4404–4414. doi:10.1182/blood-2010-05-285353
15. Fang RZ, Xu J, Lin H, Xu XG, Tian F. The histone demethylase lysine-specific demethylase-1-mediated epigenetic silence of KLF2 contributes to gastric cancer cell proliferation, migration, and invasion. *Tumor Biol*. 2017;39(4):Apr. doi:10.1177/1010428317698356
16. Tetreault MP, Yang Y, Katz JP. Kruppel-like factors in cancer. *Nat Rev Cancer*. 2013;13(10):701–713. doi:10.1038/nrc3582
17. Yin H, Xue W, Chen S, et al. Genome editing with Cas9 in adult mice corrects a disease mutation and phenotype. *Nat Biotechnol*. 2014;32(6):551–553. doi:10.1038/nbt.2884
18. Hanahan D, Weinberg RA. Hallmarks of cancer: the next generation. *Cell*. 2011;144(5):646–674. doi:10.1016/j.cell.2011.02.013
19. Roberta D, Romiti A, Milione M, et al. Somatostatin receptor subtype 2 expression in gastric cancer: an immunohystochemical study. *Ann Oncol*. 2009;20.
20. Hu CY, Yi CQ, Hao ZM, et al. The effect of somatostatin and SSTR3 on proliferation and apoptosis of gastric cancer cells. *Cancer Biol Ther*. 2004;3(8):726–730. doi:10.4161/cbt.3.8.962
21. Ricketts CJ, Morris MR, Gentle D, et al. Genome-wide CpG island methylation analysis implicates novel genes in the pathogenesis of renal cell carcinoma. *Epigenetics-Us*. 2012;7(3):278–290. doi:10.4161/epi.7.3.19103
22. Housden BE, Perrimon N. Comparing CRISPR and RNAi-based screening technologies. *Nat Biotechnol*. 2016;34(6):621–623. doi:10.1038/nbt.3599
23. Ran FA, Hsu PD, Lin CY, et al. Double nicking by RNA-guided CRISPR Cas9 for enhanced genome editing specificity (vol 154, pg 1380, 2013). *Cell*. 2013;155(2):479–480. doi:10.1016/j.cell.2013.09.040
24. Saxton RA, Sabatini DM. mTOR signaling in growth, metabolism, and disease. *Cell*. 2017;168(6):960–976. doi:10.1016/j.cell.2017.02.004
25. Matsuoka T, Yashiro M. The role of PI3K/Akt/mTOR signaling in gastric carcinoma. *Cancers*. 2014;6(3):1441–1463. doi:10.3390/cancers6031441
26. Parsons SL, Watson SA, Collins HM, Griffin NR, Clarke PA, Steele RJ. Gelatinase (MMP-2 and −9) expression in gastrointestinal malignancy. *Br J Cancer*. 1998;78(11):1495–1502. doi:10.1038/bjc.1998.712
27. Zou KL, Lu XJ, Ye K, Wang CM, You TG, Chen JL. Kruppel-like factor 2 promotes cell proliferation in hepatocellular carcinoma through up-regulation of c-myc. *Cancer Biol Ther*. 2016;17(1):20–26. doi:10.1080/15384047.2015.1108484